HHS Public Access

Author manuscript

Circ Res. Author manuscript; available in PMC 2022 November 12.

Published in final edited form as:

Circ Res. 2021 November 12; 129(11): 992–1005. doi:10.1161/CIRCRESAHA.120.318479.

SMC Derived Hyaluronan Modulates Vascular SMC-Phenotype in Murine Atherosclerosis

Felicia Hartmann[1,#], **Daniel J Gorski**[1,#], **Alexandra A. C. Newman**[2,3,4], **Susanne Homann**[1], **Anne Petz**[1], **Katherine M. Owsiany**[2,3], **Vlad Serbulea**[2], **Yu-Qing Zhou**[5], **Rebecca A. Deaton**[2], **Michelle Bendeck**[5], **Gary K Owens**[2,§], **Jens W Fischer**[1,§]

[1.]Institute of Pharmacology and Clinical Pharmacology, Medical Faculty, Heinrich-Heine-University Düsseldorf, Düsseldorf, Germany

[2.]Robert M. Berne Cardiovascular Research Center, University of Virginia-School of Medicine, Charlottesville, VA, USA

[3.]Department of Biochemistry and Molecular Genetics, University of Virginia-School of Medicine, Charlottesville, VA, USA

[4.]Cardiovascular Research Center in the Department of Medicine, New York University, New York, NY, USA

[5.]Department of Laboratory Medicine and Pathobiology, University of Toronto, Toronto, Ontario, Canada.

Abstract

Rationale: Plaque instability remains poorly understood and new therapeutic approaches to reduce plaque rupture and subsequent clinical events are of great interest. Recent studies revealed an important role of phenotypic switching of smooth muscle cells (SMC) in controlling plaque stability, including extracellular matrix (ECM) deposition.

Objective: The aim of this study was to elucidate the role of hyaluronan (HA) derived from SMC-HA synthase 3 (*Has3*), in phenotypic switching and plaque stability in an animal model of atherosclerosis.

Methods and Results: A mouse line with SMC-specific deletion of *Has3* and simultaneous SMC lineage tracing (*e*YFP) on an *Apoe*$^{-/-}$ background was used. Lineage tracing of SMC with *e*YFP revealed that SMC-specific deletion of *Has3* significantly increased the number of galectin-3 (LGALS3^{+}) “transition-state” SMC and decreased alpha-smooth muscle actin (ACTA2^{+}) SMC. Notably, SMC-*Has3* deletion led to significantly increased collagen deposition

Address correspondence to: Dr. Jens W. Fischer, Institute of Pharmacology and Clinical Pharmacology, University Hospital of the Heinrich-Heine-University Düsseldorf, Moorenstraße 5, 4022, Düsseldorf, Germany, jens.fischer@uni-duesseldorf.de.
[#]Equally contributed
[§]Equally contributed

DISCLOSURES
None.

and maturation within the fibrous cap (FC) and the whole lesion, as evidenced by Picrosirius red staining and LC-PolScope analysis. Single-cell RNA sequencing (scRNA-seq) of brachiocephalic artery (BCA) lesions demonstrated that the loss of SMC-*Has3* enhanced the transition of SMC to an *Lgals3*$^{+}$, ECM-producing phenotype with elevated acute-phase response gene expression. Experiments using cultured murine aortic SMC revealed that blocking cluster of differentiation-44 (CD44), an important HA binding receptor, recapitulated the enhanced acute-phase response and synthesis of fibrous ECM.

Conclusions: These studies provide evidence that the deletion of SMC-*Has3* results in an ECM-producing "transition state" SMC phenotype (characterized by LGALS3^{+} expression), likely via reduced CD44 signaling, resulting in increased collagen formation and maturation, an index consistent with increased plaque stability.

Graphical Abstract

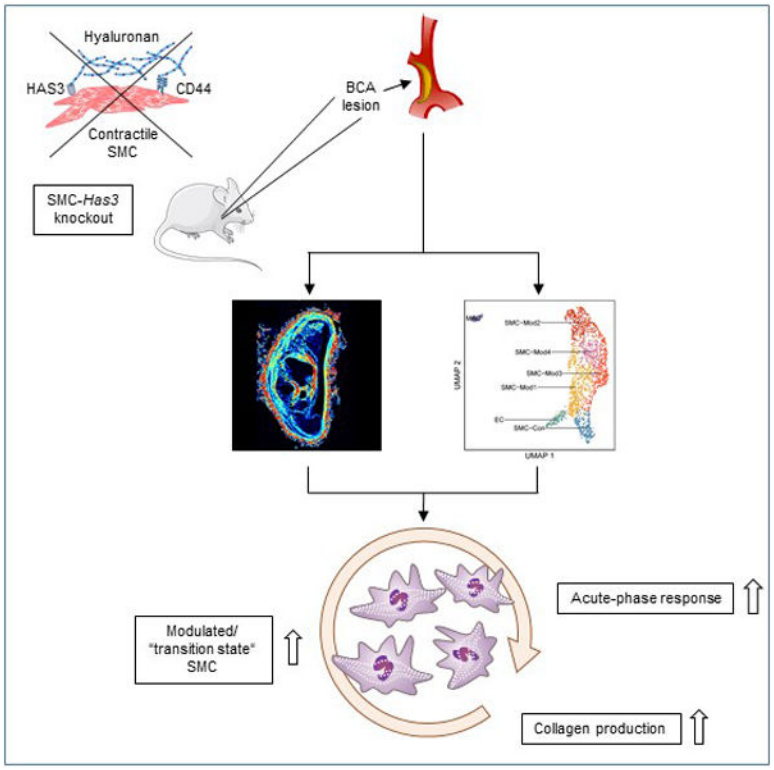

Subject Terms:

Animal Models of Human Disease; Atherosclerosis; Cell Biology/Structural Biology; Smooth Muscle Proliferation and Differentiation; Vascular Biology

INTRODUCTION

Atherosclerosis and subsequent thromboembolic complications of ruptured or eroded lesions result in myocardial infarction and stroke. A collagen-rich fibrous cap (FC) is thought to play a crucial role in stabilizing atherosclerotic lesions, whereas unstable lesions,

characterized by a thinner FC, are more prone to rupture[1–3]. *Newman et al.* recently showed that multiple cell types give rise to alpha-smooth muscle actin (ACTA2$^+$) FC cells[4]. However, SMC are the most abundant source and appear to be required for extracellular matrix (ECM) deposition and long-term durable plaque stability. To form the FC, SMC undergo phenotypic modulation in response to atherogenic stimuli and migrate from the media into atherosclerotic lesions[5–7]. Recent lineage tracing studies in mice revealed that SMC can be beneficial or detrimental in atherosclerotic lesions, depending on the specific SMC phenotypic transitions[7–13]. For example, KLF4-dependent transitions appear to be detrimental, as SMC-*Klf4* knockout (KO) resulted in a 50% decrease in lesion size but a near doubling of the thickness of the FC per lesion area[9]. In contrast, SMC-*Oct4* KO resulted in larger lesions that had multiple features of decreased plaque stability including reduced numbers of ACTA2$^+$ SMC within the FC[10]. Up to 80% of phenotypically modulated SMC within the lesion lose their typical marker genes like ACTA2 and often express galectin-3 (LGALS3), initially thought to mark the transition of SMC to a terminal macrophage-like state, especially within the lesion core[9, 11, 14, 15]. However, subsequent reports and combined lineage tracing and single-cell RNA sequencing (scRNA-seq) studies[7, 8, 12, 13] showed that the majority of LGALS3$^+$ SMC represent unique “transition state” phenotypes. Indeed, using micro-dissected lesions isolated from a novel *Myh11*-DreER^{T2}-*Lgals3*-Cre dual recombinase mouse model system, *Alencar et al.* showed that *Lgals3* mRNA expression marks this SMC “transition state” that gives rise to at least 4–5 distinct transcriptomic clusters[7]. Similarly, *Wirka et al.* recently defined a single putative beneficial ECM-producing SMC phenotype, so called a fibromyocyte, that expresses *Lgals3*[8]. Additionally, *Pan et al.* revealed multiple *Lgals3* expressing cell types derived from SMC in human and mouse lesions, including an intermediate cell state positive for stem cell, endothelial cell (EC) and macrophage markers[12]. They further showed that transitions back to a contractile SMC state might occur. Our aim, herein, was to better understand the ECM-SMC cross talk that regulates SMC populations and their functions within the lesion in order to promote beneficial (plaque stabilizing) changes in SMC phenotype and/or inhibit detrimental changes.

An interesting candidate for ECM mediated phenotypic modulation is hyaluronan (HA). It has indeed been shown that HA is important in atherosclerosis and in controlling lesion characteristics. HA is a linear unbranched glycosaminoglycan that is synthesized by SMC and other cells during atherosclerotic lesion development[16]. It is directly extruded into the extracellular space by three transmembrane HA synthases, HAS1–3, where it contributes to the matrix microenvironment of cells and acts as a direct signaling agent via HA-binding receptors. One of its most important receptors is cluster of differentiation-44 (CD44), which is thought to contribute to macrophage-induced inflammation during development of atherosclerosis[17, 18].

While HA is found and synthesized mainly in the adventitia in the healthy arterial vessel wall by fibroblasts and SMC, it has become clear that many different cells such as T-cells, macrophages, and endothelial cells contribute to the vascular HA matrix. Adding to the complex and highly variable HA-microenvironment, HA receptors including CD44 and HA-binding molecules are expressed by a variety of cell types[19] often found within the atherosclerotic lesion milieu. Both in the injured or atherosclerotic vessel and *in vitro*,

it has been shown that HA directly influences the behavior of SMC by promoting their migration and proliferation[20]. This activation of HA synthesis-induced expansion of SMC is suggested to contribute to re-stenosis and development of atherosclerotic lesions[20, 21]. In contrast, endothelial HA, a part of the glycocalyx, contributes to the protective function of the endothelium with loss of endothelial HA leading to endothelial dysfunction[22]. Given the physiological relevance of HA and HAS in atherosclerotic development, it is important to define the role of the different HAS-isoenzymes and the cellular origin in lesion development. *Has3* drives neointimal hyperplasia[23] and has been shown to be the most strongly induced HAS-isoenzyme during early atherosclerotic lesion development in mice[24]. Using global *Has3*$^{-/-}$ mice on an *Apoe*$^{-/-}$ background, we previously showed that global loss of *Has3* decreased Th1-cell polarization and subsequently, macrophage-driven plaque inflammation, resulting in an overall beneficial plaque phenotype[24].

In this study, we used a combinatorial SMC-lineage tracing and SMC-specific *Has3* KO approach to investigate the role of SMC-derived *Has3* expression and HA on SMC phenotypic modulation during development and progression of atherosclerosis in mice.

METHODS

Data Availability.

The data that support the findings of this study are available from the corresponding author upon reasonable request.

Mice, lineage tracing, and study design.

Myh11-CreER^{T2} ROSA26-STOP floxed *e*YFP *Apoe*$^{-/-}$ *Has3*$^{fl/fl}$ mice (henceforth: SMC-*Has3* WT / SMC-*Has3* KO, Suppl. Fig. I A) were generated by crossing *Myh11*-CreER^{T2} ROSA26-STOP floxed *e*YFP *Apoe*$^{-/-}$ mice[7, 9, 10, 25] with *Has3*$^{fl/fl}$ mice[23, 24] to create a SMC-specific *Has3* deficiency and simultaneous lineage tracing in SMC by *e*YFP expression. To induce the CreER^{T2} recombinase under the control of the *Myh11* promoter, expressed exclusively by SMC and a subset of microvascular pericytes[25, 26], 5–7 week old mice were given a series of 10 intraperitoneal tamoxifen injections (1 mg/day per mouse) over two weeks as previously described[7, 9, 10, 25]. At the time of labeling within the healthy vessel, the activation of the YFP reporter gene and the *Has3* excision corresponds exclusively to the vascular SMC population in the media, these events are permanent and independent of *Myh11* expression levels at later time points. Three days after the treatment, the mice were fed a western-type diet for 15 weeks, containing 21% butter fat and 0.15% cholesterol (Ssniff, S8200-E010, Suppl. Fig. I B). This system allows the identification of all progeny of medial SMC by *e*YFP expression even after accumulating within the lesion and losing their specific marker genes under pathological conditions. Hypercholesterolemia was defined as plasma cholesterol levels >500 g/dL. All animal protocols were approved by the *University of Virginia Animal Care and Use Committee* and the *Landesamt für Natur, Umwelt und Verbraucherschutz (LANUV) Nordrhein-Westfalen, Bezirksregierung Düsseldorf.*

Single-cell RNA sequencing.

Single-cell capture and library preparation were performed at the *Genome Analysis and Technology Core, RRID:SCR_018883 of the University of Virginia,* as previously described[7]. Cells were isolated and pooled from advanced lesions by micro-dissection of the BCA plaque from 5 SMC-*Has3* WT and 6 SMC-*Has3* KO mice, after 15 weeks of western diet feeding. Samples were then processed using the 10x Genomics Chromium platform. Sequencing was performed on an Illumina NextSeqTM, 150 cycle high output. Quality control was conducted by Qubit and Agilent DNA high sensitivity tape stations after 10x library prep and NGS library prep. Data analysis was performed in R version 3.6.1, using the Seurat package version 3.1.5[27]. Integration and normalization were performed using the combined SCTransform and integration workflow of Seurat as described before[28, 29]. Gene ontology term and Reactome pathway over-representation analysis was performed using a PANTHER powered web-service, http://geneontology.org/[30]. Interaction networks were generated and exported using the STRING v11 web-service, https://string-db.org/[31]. The figures, including enrichment plots, were generated with ggplot2[32, 33]. Full details can be found in the supplemental materials. Please see the Major Resources Table in the supplemental materials.

RESULTS

SMC-Has3 regulates SMC phenotype and modulates plaque composition during atherosclerosis.

To determine the effect of SMC-specific *Has3* KO on atherosclerotic lesion development, we generated a mouse model combining tamoxifen-inducible SMC-specific *Has3* deletion and simultaneous SMC-lineage tracing by *e*YFP expression under the control of the SMC-specific *Myh11* promoter (see Methods, Suppl. Fig. I A). SMC-*Has3* WT and SMC-*Has3* KO mice were fed a western-type diet for 15 weeks to induce advanced atherosclerotic lesions (Suppl. Fig. I B). All mice were genotyped and a sufficient knockdown of *Has3* as well as induction of *e*YFP expression in SMC was validated (Suppl. Fig. II). Body weight, plasma cholesterol, and plasma triglycerides were not affected by the SMC-*Has3* KO (Suppl. Fig. III). To test if SMC-*Has3* KO reduced overall HA abundance within lesions, we performed HA affinity-histochemistry and observed a significant reduction of HA in SMC-*Has3* KO mice (Suppl. Fig. IV). To elucidate the effects of SMC-*Has3* KO, the lesion cell composition was analyzed by high-resolution z-stack confocal microscopy using *e*YFP as a lineage tracing marker for SMC origin, as well as ACTA2 and LGALS3 (Fig. 1). Whereas the latter two markers do not rigorously define distinct SMC-derived lesion phenotypes[7], they represent critical SMC-derived subsets and enable us to compare our results to those described in previous publications in the field[7–9, 12]. SMC-*Has3* KO mice did not show statistically significant differences in the percentage of *e*YFP$^+$ SMC compared to SMC-*Has3* WT within the lesion core or FC (defined as the 30 μm thick, subluminal portion of the lesion[4]). However, notably, lesions of SMC-*Has3* KO mice contained significantly fewer ACTA2$^+$ SMC and showed marked increases in LGALS3$^+$ SMC within the lesion core (Fig. 1 C) and the FC (Fig. 1 D). These data indicate that SMC-*Has3* KO has a major influence on SMC phenotypic transitions within advanced atherosclerotic lesions.

SMC-Has3 deletion increases BCA lesion collagen content and maturation.

We next investigated if the observed changes in proportion of SMC phenotypes resulted in changes in multiple indices of plaque stability. We investigated lesion morphology at three well-defined locations along the BCA. SMC-*Has3* KO mice showed no statistically significant differences in lesion area, necrotic core area, or overall aortic plaque burden as compared to littermate WT control mice (Suppl. Fig. V A and B). We then tested intraplaque hemorrhage by TER119 staining and similarly found no significant difference between SMC-*Has3* KO and SMC-*Has3* WT mice (Suppl. Fig. VI). Since we observed a decreased percentage of ACTA2$^+$ SMC in the lesion core and FC, we next assessed collagen deposition by Picrosirius red staining. Unexpectedly, we observed markedly increased collagen deposition in SMC-*Has3* KO mice compared to SMC-*Has3* WT mice at three locations along the BCA (Fig. 2 A). Moreover, in-depth characterization of collagen maturation by LC-PolScope analysis[34–36], that is defined as indicative of increased organization and cross-linking to form aligned collagen fibers, revealed that SMC-*Has3* KO did not only influence collagen deposition and fibrillar collagen content, it also increased the average birefringence retardance (Fig. 2 B). Collagen organization into thick, aligned fibers in a tissue results in birefringence that retards plane polarized light. Thus, an increase in retardance corresponds to increased organization and cross-linking to form aligned collagen fibers and is indicative of both increased collagen content and maturation in the SMC-*Has3* KO. Further characterization of fiber thickness showed that SMC-*Has3* KO lesions also had increased thick collagen fibers, with no change in thin fiber deposition (Suppl. Fig. VII) within the lesion core and FC. This more matured fibrillar collagen matrix is thought to contribute to greater plaque stability[37]. To further understand ECM maturation and organization status, we assessed deposition of the collagen assembly proteoglycan decorin and found it was also increased in SMC-*Has3* KO atherosclerotic lesions (Suppl. Fig. VIII). Decorin is a small leucine-rich proteoglycan (SLRP) that connects collagen type I fibrils and plays a key role in collagen fibrillogenesis[38, 39]. Taken together, the increased collagen deposition, fibrillar collagen thickness, maturation, and organization, suggest that SMC-*Has3* KO is associated with changes in the extracellular matrix milieu consistent with increased plaque stability despite reductions in the percentage of ACTA2$^+$ SMC within the FC[37].

scRNA-seq characterization of BCA lesions reveals 5 distinct SMC clusters.

To gain further insight into the role of SMC-*Has3* in atherosclerotic lesion development, we performed scRNA-seq on plaques from 5 SMC-*Has3* WT and 6 SMC-*Has3* KO mice after 15 weeks of western diet. Briefly, advanced lesions were micro-dissected from the BCA, sorted for *e*YFP$^+$ cells, and processed using a 10x Genomics Chromium platform. Transcriptomes from 1,600 cells were used after quality control filtering. SMC-*Has3* WT and KO data sets were integrated and the cell identities were profiled together by clustering using the *Seurat* package[27]. We found 7 distinct populations of lesion cells, including endothelial cells (EC; *Pecam1*$^+$, *Cdh5*$^+$), macrophages (MAC; *Ptprc*$^+$, *Cd68*$^+$, *Adgre1*$^+$, *Fcgr1*$^+$, *Itgam*$^+$, *Mrc1*$^+$), contractile SMC (SMC-Con; *eyfp*$^+$, *Myh11*$^+$, *Acta2*$^+$, *Tagln*$^+$) and 4 modulated SMC clusters characterized by *Lgals3* expression (SMC-Mod1–4; *eyfp*$^+$, *Lgals3*$^+$, *Tnfrsf11b*$^+$, *Lum*$^+$, *Spp1*$^+$, *Myh11*$^-$, *Acta2*$^-$, *Tagln*$^-$). These observed clusters are consistent with a recently published larger dataset by our group[7]. SMC-Con and SMC-

Mod1–4 clusters were confirmed to be from SMC lineage by mRNA *eyfp* expression, which was absent in the endothelial cell and macrophage clusters (Fig. 3 A–C, Suppl Fig IX). The presence of *Lgals3* expression and absence of canonical macrophage markers (*Adgre1, Cd68, Fcgr1,* and *Itgam)* in modulated SMC clusters is in agreement with recent scRNA-seq reports[7, 8, 12, 13] showing that *Lgals3* expression marks a SMC transition state rather than a terminal macrophage-like state. The majority of SMC in this analysis had acquired a transition state, including cells in the SMC-Con cluster, which express both contractile marker genes (e.g., *Acta2* and *Myh11*) as well as *Lgals3,* albeit at a lower level than SMC-Mod clusters. This gene expression profile may suggest that these SMC are poised to undergo phenotypic switching (Fig. 3 B) or have transitioned back to a semi-contractile state, as they were distinct from the modulated state. Gene expression signatures of fibrillar collagens and SLRPs were elevated in the SMC-Mod clusters compared to SMC-Con (Fig. 3 B, Supplemental Files 1,7), indicating that SMC-Mod express a higher amount of collagen and collagen fiber assembly machinery. Differential gene expression analysis also supported the observation that SMC-Mod clusters exhibited an ECM-synthesizing phenotype, as the ECM genes *Acan, Col2a1, Hapln1, Col27a1, Col11a2, Col6a1, Sparc, Fmod* and *Dcn*, among others, were significantly upregulated compared to SMC-Con (Suppl. Fig. X, Supplemental File 3).

By identifying cluster marker genes (Supplemental File 4) and analyzing their gene ontology (GO) enrichment (Suppl. Fig. XI) the 4 sub-populations of modulated SMC clusters can be generally described as collagen producing (SMC-Mod1), osteochondrogenic (SMC-Mod2), inflammatory (SMC-Mod3), and growth factor responsive (SMC-Mod4). Specifically, SMC-Mod1 exhibited high expression of *Col1a1, Col3a1, Col5a2, Col6a1, and Col6a3* and had an overrepresentation of genes belonging to ECM-related GO terms like “extracellular matrix organization” and “endochondral bone growth” (Suppl. Fig. IX and XI). SMC-Mod2 expressed chondrogenic marker genes, *Hapln1, Acan, and Col2a1* and exhibited enrichment of genes associated with GO terms like “cartilage development”, “chondrocyte differentiation”, and “bone mineralization”. SMC-Mod2 may also exhibit an osteochondrogenic phenotype, which was supported by high expression of Integrin Binding Sialoprotein (*Ibsp*), a major component of bone matrix. SMC-Mod3 likely represents a modulated SMC population devoted to inflammatory cell interactions as it expressed *Lcn2, C3,* and *Lbp* at high levels, all of which are involved in innate immunity and the acute-phase response. SMC-Mod3 marker genes also had an overrepresentation of genes belonging to the GO terms like “inflammatory response” and “defense response”. Lastly, SMC-Mod4, exhibited a high expression of transcription and growth factors like *Jun, Egr1,* and *Gdf10* and was enriched for genes belonging to GO terms related to differentiation and response to growth factors/cytokines.

scRNA-seq demonstrates SMC-Has3 deletion promotes modulated SMC phenotypes and elevates the acute-phase response.

Overall, scRNA-seq profiling of advanced BCA lesions from SMC-*Has3* KO mice showed a greater abundance of modulated SMC and fewer contractile SMC as compared to SMC-*Has3* WT lesions (Fig. 4 A and B). This shift towards the modulated SMC phenotype revealed by scRNA-seq also supports the immunohistochemical analysis that demonstrated a

greater abundance of LGALS3$^+$ SMC within the lesion and FC and reduced ACTA2$^+$ SMC (Fig. 1). To examine the modulated SMC state as a whole, we grouped the modulated SMC clusters together and performed differential gene expression analysis between SMC-*Has3* KO and SMC-*Has3* WT mice (Fig. 4 C, Supplemental File 5). Significant and highly upregulated genes in modulated SMC from SMC-*Has3* KO mice included *Lcn2*, *Saa1*, *Saa2, Saa3*, *C3* and *Hp* among others. Upregulated genes were examined for overrepresentation of GO terms and showed an enrichment of genes belonging to “acute-phase response”, “inflammatory response”, “response to bacterium”, as well as GO terms involving metal ion homeostasis (Fig. 4 D). Differential gene expression analysis between SMC-*Has3* KO and SMC-*Has3* WT cells was also performed within each individual cluster and the significantly upregulated genes were examined with interaction networks to uncover common pathways and functions (Suppl. Fig. XII, Supplemental File 6). SMC-*Has3* KO cells in the SMC-Mod1 and SMC-Mod2 clusters had elevated expression of defense response genes including (*Chil1*, *Hp*, *Lcn2*, *Lbp*, *C3*, *C1s1*, *Hmgb2*, *Dbi*, *Prdx1*, *Ifitm2,* and *Cebpb).* The inflammatory sub-population (SMC-Mod3) had the largest amount of significantly regulated genes. Upregulated genes in the SMC-Mod3 group of SMC-*Has3* KO mice were involved in the acute-phase response (*Lcn2*, *Saa1*, *Saa2*, *Saa3,* and *Lbp)* and collagen biosynthesis and crosslinking (*Col2a1*, *Col9a3*, *Col11a2,* and *Plod2*).

Acta2 and ECM gene expression can be modulated by in vitro Has3 knockdown or blocking CD44 in cultured aortic SMC.

Next, *in vitro* experiments were performed to identify mechanistic pathways that mediate the altered SMC response in the absence of *Has3*. It has been postulated that HAS3 synthesizes a lower molecular weight HA compared to HAS1 and HAS2[40] and that low molecular weight HA may illicit inflammatory responses, although these claims have been challenged[41]. Therefore, we sought to better characterize the present HA species and the specific contribution of HAS3 in murine SMC. Lineage traced murine *e*YFP$^+$ aortic SMC cultures were established and incubated for 48 hours with 10 ng/mL rhPDGF-BB and 10 ng/mL mTGF-β1 to induce an activated, matrix producing state[4]. After incubation, cells were treated with either siRNA targeting *Has3* (si*Has3*) or non-targeting siRNA (siNT) or CD44 blocking antibody/isotype control or a combined treatment of both. We did not observe statistically significant morphological differences due to the siRNA or antibody treatment (Fig. 5 A). Administration of *Has3* siRNA resulted in a significant reduction of HA in the cell culture supernatant and reduced *Has3* expression by 70% without a compensatory increase in *Has1* or *Has2* expression (Fig. 5 B, C). Using agarose gel electrophoresis, we determined the molecular mass distribution of the HA present by loading equal amounts of secreted HA isolated from siNT and si*Has3* treated cells. This demonstrated that the HA in the present system is of intermediate to high molecular weight (300 kDa – 2+ MDa) and the *Has3* silenced SMC have a modest shift towards higher molecular weight HA (Fig. 5 D). Hyaluronidase (*Hyal*) gene expression and hyaluronidase activity were also profiled. *Hyal2* expression was significantly upregulated and hyaluronidase activity demonstrated a subtle, but not statistically significant increase (Fig. 5 E, F). This is likely inconsequential, as there was rather a small increase in molecular mass distribution (Fig. 5 D). Additionally, CD44 splice variant expression was analyzed, SMC largely expressed the standard variant (CD44s) (Suppl. Fig. XIII).

Consistent with our *in vivo* observations in this model, *Has3* targeted siRNA treatment as well as CD44 blocking significantly reduced *Acta2* expression (Fig. 6 A). Moreover, si*Has3* treatment and CD44 blocking increased fibrillar collagen *Col1a1*, as well as the ECM organizing collagen *Col15a1.* In addition, *Col3a1* and *Fn1*, both already known to be induced in SMC transition states[7, 8, 12], were increased in si*Has3* and CD44 blocked samples (Fig. 6 B). Combined treatment of si*Has3* and CD44 blocking did not show additive effects. These *in vitro* investigations support the *in vivo* findings outlined in this study and suggest that increased SMC phenotypic switching after SMC-*Has3* KO may be driven by decreased HA/CD44 signaling, as blocking CD44 reproduced the *Has3* KD phenotype.

CD44 blocking induces the acute-phase response in murine SMC.

To further evaluate the role of CD44 we profiled the acute-phase response in murine aortic SMC after CD44 blocking, as this was a highly upregulated pathway identified by scRNA-seq. Indeed, CD44 blocking strongly upregulated the expression of acute-phase response genes; *Lcn2, Saa3* and *Hp* (Fig. 7 A). As well as secretion of LCN2 into the supernatant (Fig. 7 B). CD44 blocking also led to the statistically significant increase of *Col1a1* and *Dcn* expression (Fig. 6 C). Inhibiting NF-κB nuclear translocation by the addition of specific inhibitor, JSH-23, diminished the upregulation of *Lcn2* (Fig. 7 D), suggesting at least a partial involvement of the NF-κB pathway. It has been previously shown that Serum Amyloid A and LCN2 can drive phenotypic switching[42, 43]. To confirm their potential to drive SMC modulation we stimulated our murine SMC cultures with recombinant LCN2 and Apo-SAA and found that their addition significantly upregulated *Col1a1* and *Dcn* and downregulated *Acta2* expression respectively (Fig. 7 E).

DISCUSSION

In recent years, the HA matrix has been shown to fulfill diverse functions in the context of cardiovascular diseases. In addition to facilitating neointimal matrix expansion and SMC migration[20, 21], an immunomodulatory function and an important role in endothelial (dys)function has been shown[22, 24]. It is also known that T-cell responses are modulated by HA based on its function in the T-cell immune synapse to reduce Th1 cell polarization[24]. In addition, in the context of recovery after myocardial infarction, it has been shown that HA increases macrophage survival and myofibroblast responses in mice[44].

The aforementioned studies highlight the divergent, and in part, opposing roles of HA in different functional organ compartments and in different cell types. Therefore, in this study we aimed to unravel the role of HAS3 expression by SMC in atherosclerosis development. Ubiquitous, constitutive deletion of *Has3* in *Apoe*$^{-/-}$ mice reduced Th1 cell polarization, resulting in reduced macrophage driven inflammation, reduced lesion size and atheroprogression[24]. Here, loss of SMC-*Has3* did not affect lesion size or macrophage accumulation. But notably, *Has3* deficiency in SMC had a profound effect on phenotypic switching of SMC and composition of lesion ECM. Specifically, SMC-*Has3* KO reduced the percentage of ACTA2^{+} SMC within the lesion by 50% with a concomitant increase in LGALS3^{+} SMC within the lesion and FC. These results indicate an important role of SMC-*Has3* with respect to overall lesion composition and indices of plaque stability.

Therefore, it appears that HAS3 has two detrimental roles in atherosclerosis: (i) promoting Th1 cell response and macrophage accumulation and (ii) inhibiting the transition of SMC to an ECM synthesizing and plaque stabilizing phenotype.

Recently, *Alencar et al., Pan et al.,* and *Wirka et al.*[7, 8, 12] demonstrated that *Lgals3* is not a marker of a terminally differentiated SMC-derived macrophage-like cell state as previously thought[9, 11, 45] but rather represents the transition of contractile cells into an ECM remodeling pioneer cell phenotype[7, 8, 12, 13]. Moreover, they showed that the majority of SMC-derived cells in advanced BCA lesions express and likely go through an *Lgals3*$^+$ transition state from which, depending on environmental cues, SMC proceed to phenotypically modulated SMC that can either be beneficial or detrimental for lesion pathogenesis. Of major significance, results of the present study show that the loss of SMC-specific *Has3*, while resulting in an increased fraction of LGALS3$^+$ SMC and decreased ACTA2$^+$ SMC, surprisingly appears to promote beneficial changes within lesions including significantly more decorin and collagen deposition as well as collagen maturation in the FC and lesion core.

Our scRNA-seq analysis of isolated plaque lesions, which identified 5 distinct SMC populations, enabled further insight into the phenotypic status of SMC in SMC-*Has3* KO mice and possible underlying mechanisms. Consistent with *Alencar et al.*, *Pan et al.* and *Wirka et al.*, the modulated SMC populations were positive for markers associated with SMC transition, as *Lgals3, Lum, Fn1 or Tnfrsf11b*[7, 8, 12]. These observations agree with previous results, which demonstrated that 80% of lesion SMC lose their traditional, contractile marker proteins under pathological conditions such as atherosclerosis[9].

In general, inflammation develops due to its essential and beneficial roles in tissue damage repair and pathogen resistance. However, in atherosclerosis, inflammatory responses and especially macrophage driven plaque inflammation, drive atherogenesis and progression. But notably, certain pathways associated with inflammation have recently been shown to play a beneficial role in atherosclerosis. This is shown in a study on the role of IL1- and IL1R1-signal transduction in SMC phenotype and collagen deposition in atherosclerosis[46]. Although the IL1R1 signaling pathway in SMC has been shown to exacerbate the development of atherosclerosis, paradoxically, it also plays a critical role in promoting the formation and maintenance of a protective FC. Here we found that in addition to collagen, inflammatory genes involved in the acute-phase response; *Saa1, 2,* and *3*, and *Lcn2,* among others were upregulated in *Has3*-deficient SMC-modulated clusters as well as *in vitro* after CD44 blocking. Acute-phase proteins Serum amyloid A and LCN2 have been shown to promote SMC phenotypic switching[42] and collagen deposition in experimental atherosclerosis[43]. To confirm their potential to drive SMC modulation we stimulated our murine SMC cultures with recombinant Apo-SAA and LCN2. This treatment indeed stimulated *Col1a1* and *Dcn* and downregulated *Acta2.* Decorin is interesting because it is known to promote collagen fibrillogenesis and collagen matrix stability which has been shown originally in the skin by knock out[39] but also in the vasculature by overexpression[47]. Our results also indicate that CD44, one of the main HA receptors, plays a role in preventing beneficial increases in ECM deposition by suppressing the SMC expression of acute-phase proteins.

As schematically summarized in Fig. 8, LGALS3^{+} modulated SMC increase after loss of SMC-*Has3*, and likely modulate an acute-phase response, which in an autocrine manner stimulates further collagen deposition, organization, and maturation in the plaque and the FC. This effect on phenotypic switching of SMC is presumably dependent on reduced HA/CD44 signaling as suggested by experiments *in vivo* and *in vitro.* Therefore, the present results suggest strategies to inhibit SMC-*Has3*/CD44 as a possible means to increase atherosclerotic lesion stability.

Supplementary Material

Refer to Web version on PubMed Central for supplementary material.

ACKNOWLEDGEMENTS

We are grateful for the UVA genomics core facility, including Dr. Katia Sol-Church and Alyson Prorock for assistance with single-cell RNA sequencing and the UVA flow cytometry core facility, where we especially thank Michel Solga and Claude Chew for cell sorting assistance. Further we would like to thank Rupa Tripathi, Petra Pieres, Peggy Marra-Mann, Irmhild Rueter, and Beate Weyrauther for their support.

SOURCES OF FUNDING

This study was supported by the German Research Foundation (DFG), through the International research training group (IRTG) 1902 and the Comprehensive Research Center (CRC, SFB 1116) to Jens Fischer and NIH R01 grants HL136314 and HL141425 to Gary K. Owens.

Nonstandard Abbreviations and Acronyms:

4-MU	4-methylumbelliferone
ACTA2	alpha-smooth muscle actin
BCA	brachiocephalic artery
CD	cluster of differentiation
ECM	extracellular matrix
FC	fibrous cap
HA	hyaluronan
HAS	hyaluronan synthase
LGALS3	galectin-3
***e*YFP**	Enhanced yellow fluorescent protein

REFERENCES

1. Bentzon JF, Otsuka F, Virmani R and Falk E. Mechanisms of plaque formation and rupture. Circ Res 2014;114:1852–66. [PubMed: 24902970]
2. Libby P, Ridker PM and Hansson GK. Progress and challenges in translating the biology of atherosclerosis. Nature 2011;473:317–25. [PubMed: 21593864]

3. Burleigh MC, Briggs AD, Lendon CL, Davies MJ, Born GV and Richardson PD. Collagen types I and III, collagen content, GAGs and mechanical strength of human atherosclerotic plaque caps: span-wise variations. Atherosclerosis 1992;96:71–81. [PubMed: 1418104]
4. Newman AAC, Serbulea V, Baylis RA, Shankman LS, Bradley X, Alencar GF, Owsiany K, Deaton RA, Karnewar S, Shamsuzzaman S, Salamon A, Reddy MS, Guo L, Finn A, Virmani R, Cherepanova OA and Owens GK. Multiple cell types contribute to the atherosclerotic lesion fibrous cap by PDGFRbeta and bioenergetic mechanisms. Nat Metab 2021;3:166–181. [PubMed: 33619382]
5. Bennett MR, Sinha S and Owens GK. Vascular Smooth Muscle Cells in Atherosclerosis. Circ Res 2016;118:692–702. [PubMed: 26892967]
6. Gomez D and Owens GK. Smooth muscle cell phenotypic switching in atherosclerosis. Cardiovasc Res 2012;95:156–64. [PubMed: 22406749]
7. Alencar GF, Owsiany KM, K S, Sukhavasi K, Mocci G, Nguyen A, Williams CM, Shamsuzzaman S, Mokry M, Henderson CA, Haskins R, Baylis RA, Finn AV, McNamara CA, Zunder ER, Venkata V, Pasterkamp G, Bjorkegren J, Bekiranov S and Owens GK. The Stem Cell Pluripotency Genes Klf4 and Oct4 Regulate Complex SMC Phenotypic Changes Critical in Late-Stage Atherosclerotic Lesion Pathogenesis. Circulation 2020.
8. Wirka RC, Wagh D, Paik DT, Pjanic M, Nguyen T, Miller CL, Kundu R, Nagao M, Coller J, Koyano TK, Fong R, Woo YJ, Liu B, Montgomery SB, Wu JC, Zhu K, Chang R, Alamprese M, Tallquist MD, Kim JB and Quertermous T. Atheroprotective roles of smooth muscle cell phenotypic modulation and the TCF21 disease gene as revealed by single-cell analysis. Nat Med 2019;25:1280–1289. [PubMed: 31359001]
9. Shankman LS, Gomez D, Cherepanova OA, Salmon M, Alencar GF, Haskins RM, Swiatlowska P, Newman AA, Greene ES, Straub AC, Isakson B, Randolph GJ and Owens GK. KLF4-dependent phenotypic modulation of smooth muscle cells has a key role in atherosclerotic plaque pathogenesis. Nat Med 2015;21:628–37. [PubMed: 25985364]
10. Cherepanova OA, Gomez D, Shankman LS, Swiatlowska P, Williams J, Sarmento OF, Alencar GF, Hess DL, Bevard MH, Greene ES, Murgai M, Turner SD, Geng YJ, Bekiranov S, Connelly JJ, Tomilin A and Owens GK. Activation of the pluripotency factor OCT4 in smooth muscle cells is atheroprotective. Nat Med 2016;22:657–65. [PubMed: 27183216]
11. Feil S, Fehrenbacher B, Lukowski R, Essmann F, Schulze-Osthoff K, Schaller M and Feil R. Transdifferentiation of vascular smooth muscle cells to macrophage-like cells during atherogenesis. Circ Res 2014;115:662–7. [PubMed: 25070003]
12. Pan H, Xue C, Auerbach BJ, Fan J, Bashore AC, Cui J, Yang DY, Trignano SB, Liu W, Shi J, Ihuegbu CO, Bush EC, Worley J, Vlahos L, Laise P, Solomon RA, Connolly ES, Califano A, Sims PA, Zhang H, Li M and Reilly MP. Single-Cell Genomics Reveals a Novel Cell State During Smooth Muscle Cell Phenotypic Switching and Potential Therapeutic Targets for Atherosclerosis in Mouse and Human. Circulation 2020.
13. Miano JM, Fisher EA and Majesky MW. Fate and State of Vascular Smooth Muscle Cells in Atherosclerosis. Circulation 2021;143:2110–2116. [PubMed: 34029141]
14. Allahverdian S, Chehroudi AC, McManus BM, Abraham T and Francis GA. Contribution of intimal smooth muscle cells to cholesterol accumulation and macrophage-like cells in human atherosclerosis. Circulation 2014;129:1551–9. [PubMed: 24481950]
15. Wang Y, Dubland JA, Allahverdian S, Asonye E, Sahin B, Jaw JE, Sin DD, Seidman MA, Leeper NJ and Francis GA. Smooth Muscle Cells Contribute the Majority of Foam Cells in ApoE (Apolipoprotein E)-Deficient Mouse Atherosclerosis. Arterioscler Thromb Vasc Biol 2019;39:876–887. [PubMed: 30786740]
16. Evanko SP, Raines EW, Ross R, Gold LI and Wight TN. Proteoglycan distribution in lesions of atherosclerosis depends on lesion severity, structural characteristics, and the proximity of platelet-derived growth factor and transforming growth factor-beta. Am J Pathol 1998;152:533–46. [PubMed: 9466580]
17. Cuff CA, Kothapalli D, Azonobi I, Chun S, Zhang Y, Belkin R, Yeh C, Secreto A, Assoian RK, Rader DJ and Pure E. The adhesion receptor CD44 promotes atherosclerosis by mediating inflammatory cell recruitment and vascular cell activation. J Clin Invest 2001;108:1031–40. [PubMed: 11581304]

18. Kolodgie FD, Burke AP, Farb A, Weber DK, Kutys R, Wight TN and Virmani R. Differential accumulation of proteoglycans and hyaluronan in culprit lesions: insights into plaque erosion. Arterioscler Thromb Vasc Biol 2002;22:1642–8. [PubMed: 12377743]
19. Del Monte-Nieto G, Fischer JW, Gorski DJ, Harvey RP and Kovacic JC. Basic Biology of Extracellular Matrix in the Cardiovascular System, Part 1/4: JACC Focus Seminar. J Am Coll Cardiol 2020;75:2169–2188. [PubMed: 32354384]
20. Evanko SP, Angello JC and Wight TN. Formation of hyaluronan- and versican-rich pericellular matrix is required for proliferation and migration of vascular smooth muscle cells. Arterioscler Thromb Vasc Biol 1999;19:1004–13. [PubMed: 10195929]
21. Riessen R, Wight TN, Pastore C, Henley C and Isner JM. Distribution of hyaluronan during extracellular matrix remodeling in human restenotic arteries and balloon-injured rat carotid arteries. Circulation 1996;93:1141–7. [PubMed: 8653834]
22. Nagy N, Freudenberger T, Melchior-Becker A, Rock K, Ter Braak M, Jastrow H, Kinzig M, Lucke S, Suvorava T, Kojda G, Weber AA, Sorgel F, Levkau B, Ergun S and Fischer JW. Inhibition of hyaluronan synthesis accelerates murine atherosclerosis: novel insights into the role of hyaluronan synthesis. Circulation 2010;122:2313–22. [PubMed: 21098434]
23. Kiene LS, Homann S, Suvorava T, Rabausch B, Muller J, Kojda G, Kretschmer I, Twarock S, Dai G, Deenen R, Hartwig S, Lehr S, Kohrer K, Savani RC, Grandoch M and Fischer JW. Deletion of Hyaluronan Synthase 3 Inhibits Neointimal Hyperplasia in Mice. Arterioscler Thromb Vasc Biol 2016;36:e9–16. [PubMed: 26586662]
24. Homann S, Grandoch M, Kiene LS, Podsvyadek Y, Feldmann K, Rabausch B, Nagy N, Lehr S, Kretschmer I, Oberhuber A, Bollyky P and Fischer JW. Hyaluronan synthase 3 promotes plaque inflammation and atheroprogression. Matrix Biol 2018;66:67–80. [PubMed: 28987865]
25. Gomez D, Shankman LS, Nguyen AT and Owens GK. Detection of histone modifications at specific gene loci in single cells in histological sections. Nat Methods 2013;10:171–7. [PubMed: 23314172]
26. Hess DL, Kelly-Goss MR, Cherepanova OA, Nguyen AT, Baylis RA, Tkachenko S, Annex BH, Peirce SM and Owens GK. Perivascular cell-specific knockout of the stem cell pluripotency gene Oct4 inhibits angiogenesis. Nat Commun 2019;10:967. [PubMed: 30814500]
27. Butler A, Hoffman P, Smibert P, Papalexi E and Satija R. Integrating single-cell transcriptomic data across different conditions, technologies, and species. Nat Biotechnol 2018;36:411–420. [PubMed: 29608179]
28. Stuart T, Butler A, Hoffman P, Hafemeister C, Papalexi E, Mauck WM 3rd, Hao Y, Stoeckius M, Smibert P and Satija R. Comprehensive Integration of Single-Cell Data. Cell 2019;177:1888–1902 e21. [PubMed: 31178118]
29. Hafemeister C and Satija R. Normalization and variance stabilization of single-cell RNA-seq data using regularized negative binomial regression. Genome Biol 2019;20:296. [PubMed: 31870423]
30. Mi H, Huang X, Muruganujan A, Tang H, Mills C, Kang D and Thomas PD. PANTHER version 11: expanded annotation data from Gene Ontology and Reactome pathways, and data analysis tool enhancements. Nucleic Acids Res 2017;45:D183–D189. [PubMed: 27899595]
31. Szklarczyk D, Gable AL, Lyon D, Junge A, Wyder S, Huerta-Cepas J, Simonovic M, Doncheva NT, Morris JH, Bork P, Jensen LJ and Mering CV. STRING v11: protein-protein association networks with increased coverage, supporting functional discovery in genome-wide experimental datasets. Nucleic Acids Res 2019;47:D607–D613. [PubMed: 30476243]
32. Wickham H ggplot2; 2009.
33. Bonnot T, Gillard M and Nagel D. A Simple Protocol for Informative Visualization of Enriched Gene Ontology Terms. Bio-Protocol 2019;9.
34. Shribak M and Oldenbourg R. Techniques for fast and sensitive measurements of two-dimensional birefringence distributions. Appl Opt 2003;42:3009–17. [PubMed: 12790452]
35. Oldenbourg R A new view on polarization microscopy. Nature 1996;381:811–2. [PubMed: 8657288]
36. Oldenbourg R and Mei G. New polarized light microscope with precision universal compensator. J Microsc 1995;180:140–7. [PubMed: 8537959]

37. Durgin BG, Cherepanova OA, Gomez D, Karaoli T, Alencar GF, Butcher JT, Zhou YQ, Bendeck MP, Isakson BE, Owens GK and Connelly JJ. Smooth muscle cell-specific deletion of Col15a1 unexpectedly leads to impaired development of advanced atherosclerotic lesions. Am J Physiol Heart Circ Physiol 2017;312:H943–H958. [PubMed: 28283548]

38. Hocking AM, Shinomura T and McQuillan DJ. Leucine-rich repeat glycoproteins of the extracellular matrix. Matrix Biol 1998;17:1–19. [PubMed: 9628249]

39. Danielson KG, Baribault H, Holmes DF, Graham H, Kadler KE and Iozzo RV. Targeted disruption of decorin leads to abnormal collagen fibril morphology and skin fragility. J Cell Biol 1997;136:729–43. [PubMed: 9024701]

40. Itano N, Sawai T, Yoshida M, Lenas P, Yamada Y, Imagawa M, Shinomura T, Hamaguchi M, Yoshida Y, Ohnuki Y, Miyauchi S, Spicer AP, McDonald JA and Kimata K. Three isoforms of mammalian hyaluronan synthases have distinct enzymatic properties. J Biol Chem 1999;274:25085–92. [PubMed: 10455188]

41. Dong Y, Arif A, Olsson M, Cali V, Hardman B, Dosanjh M, Lauer M, Midura RJ, Hascall VC, Brown KL and Johnson P. Endotoxin free hyaluronan and hyaluronan fragments do not stimulate TNF-alpha, interleukin-12 or upregulate co-stimulatory molecules in dendritic cells or macrophages. Sci Rep 2016;6:36928. [PubMed: 27869206]

42. Zhang X, Chen J and Wang S. Serum Amyloid A Induces a Vascular Smooth Muscle Cell Phenotype Switch through the p38 MAPK Signaling Pathway. Biomed Res Int 2017;2017:4941379. [PubMed: 28642873]

43. Shibata K, Sato K, Shirai R, Seki T, Okano T, Yamashita T, Koide A, Mitsuboshi M, Mori Y, Hirano T and Watanabe T. Lipocalin-2 exerts pro-atherosclerotic effects as evidenced by in vitro and in vivo experiments. Heart Vessels 2020;35:1012–1024. [PubMed: 31960147]

44. Petz A, Grandoch M, Gorski DJ, Abrams M, Piroth M, Schneckmann R, Homann S, Muller J, Hartwig S, Lehr S, Yamaguchi Y, Wight TN, Gorressen S, Ding Z, Kotter S, Kruger M, Heinen A, Kelm M, Godecke A, Flogel U and Fischer JW. Cardiac Hyaluronan Synthesis Is Critically Involved in the Cardiac Macrophage Response and Promotes Healing After Ischemia Reperfusion Injury. Circ Res 2019;124:1433–1447. [PubMed: 30916618]

45. Rong JX, Berman JW, Taubman MB and Fisher EA. Lysophosphatidylcholine stimulates monocyte chemoattractant protein-1 gene expression in rat aortic smooth muscle cells. Arterioscler Thromb Vasc Biol 2002;22:1617–23. [PubMed: 12377739]

46. Gomez D, Baylis RA, Durgin BG, Newman AAC, Alencar GF, Mahan S, St Hilaire C, Muller W, Waisman A, Francis SE, Pinteaux E, Randolph GJ, Gram H and Owens GK. Interleukin-1beta has atheroprotective effects in advanced atherosclerotic lesions of mice. Nat Med 2018;24:1418–1429. [PubMed: 30038218]

47. Fischer JW, Kinsella MG, Levkau B, Clowes AW and Wight TN. Retroviral overexpression of decorin differentially affects the response of arterial smooth muscle cells to growth factors. Arterioscler Thromb Vasc Biol 2001;21:777–84. [PubMed: 11348874]

NOVELTY AND SIGNIFICANCE

What Is Known?

- Phenotypic modulation of smooth muscle cells (SMC) can be beneficial or detrimental to atherosclerotic lesion stability.
- Recent studies revealed an important role of galectin-3 (LGALS3)-expressing "modulated SMC" in controlling plaque stability, including inducing extracellular matrix (ECM) deposition.
- Hyaluronanic acid (HA), an important ECM component, is increased during atherosclerotic lesion progression and can directly influence SMC function by promoting SMC activation and migration.

What New Information Does This Article Contribute?

- SMC-HA synthase *(Has) 3* deficiency leads to more $LGALS3^{+}$ modulated SMC within the lesion, as well as increases collagen deposition and maturation, which are indices consistent with increased plaque stability.
- In-depth single-cell RNA sequencing demonstrates that SMC-*Has3* deletion driven expansion of phenotypically modulated SMC drives increases in acute-phase response gene expression.
- Blocking the important HA binding receptor, cluster of differentiation-44 (CD44), recapitulates the enhanced acute-phase response and synthesis of fibrous ECM.

The present studies provide evidence that SMC-*Has3* plays a crucial role for lesion stability indices by enhancing an ECM-producing "transition state" SMC phenotype which is characterized by $LGALS3^{+}$ expression, likely via reduced HA/CD44 signaling.

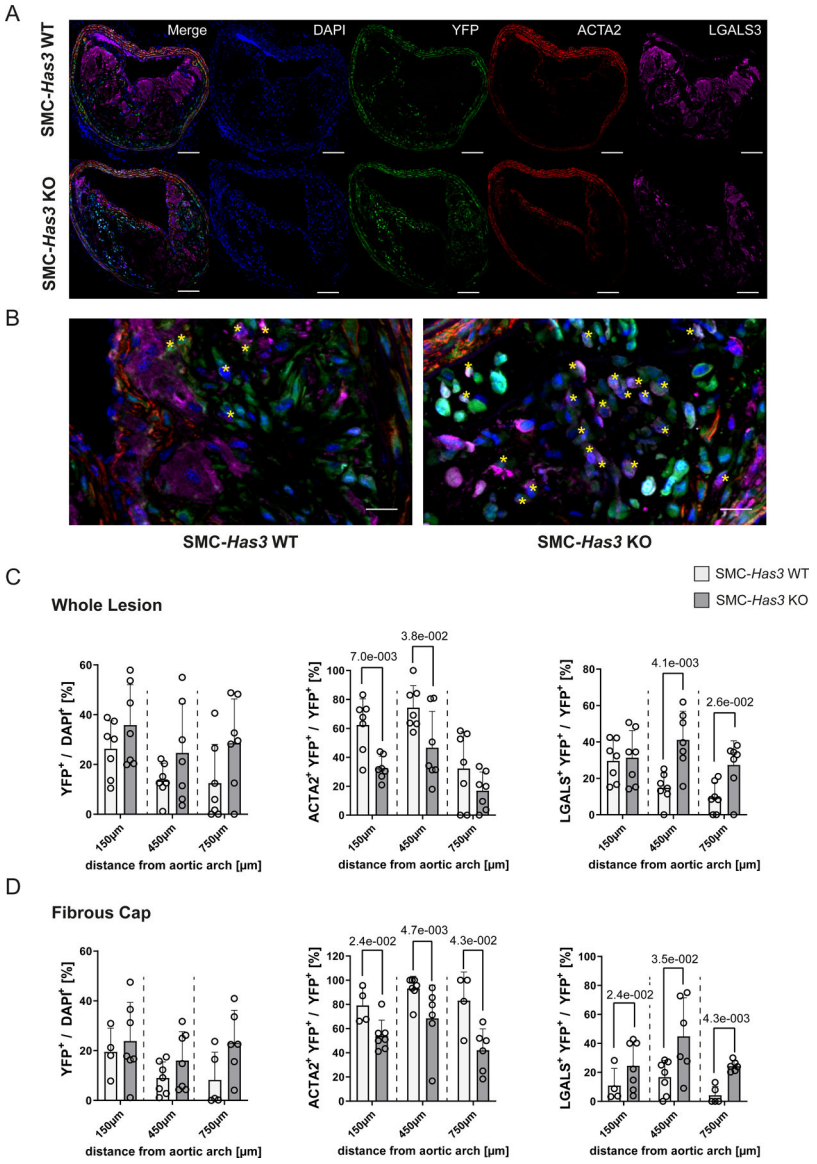

Fig. 1: Genetic deletion of SMC-*Has3* is associated with reduced SMC-derived ACTA2$^+$ and increased LGALS3$^+$ lesion cells.

(A) Immunostaining of representative BCA sections (scale bars 100 µm) of SMC-*Has3* WT and SMC-*Has3* KO mice fed a western diet for 15 weeks shows a marked increase in SMC-derived LGALS3$^+$ cells and a decrease in the number of ACTA2$^+$ SMC within lesions of SMC-specific *Has3* KO mice, as compared to control mice. **(B)** The yellow stars in higher magnification panel (scale bars 20 µm) indicates LGALS3$^+$ *e*YFP$^+$ cells in SMC-*Has3* KO mice. Quantification of *e*YFP$^+$ cells as part of total cell number (detected by DAPI signal), as well as percentages of LGALS3$^+$ *e*YFP$^+$ and ACTA2$^+$ *e*YFP$^+$ cells per *e*YFP$^+$ cells within the whole lesion (n=7/7) and **(C)** the FC (YFP$^+$/DAPI$^+$: n=4/7 (150 µm), n=7/7 (450 µm), n=5/6 (750 µm); ACTA2$^+$YFP$^+$/YFP$^+$: n=4/7 (150 µm), n=7/6 (450 µm), n=4/6 (750 µm); LGALS3$^+$YFP$^+$/YFP$^+$: n=4/7 (150 µm), n=7/6 (450 µm), n=5/6 (750 µm)) **(D)**. Statistical analysis was performed separately at three different locations along the BCA with Mann-Whitney tests. Error bars represent mean ± SD.

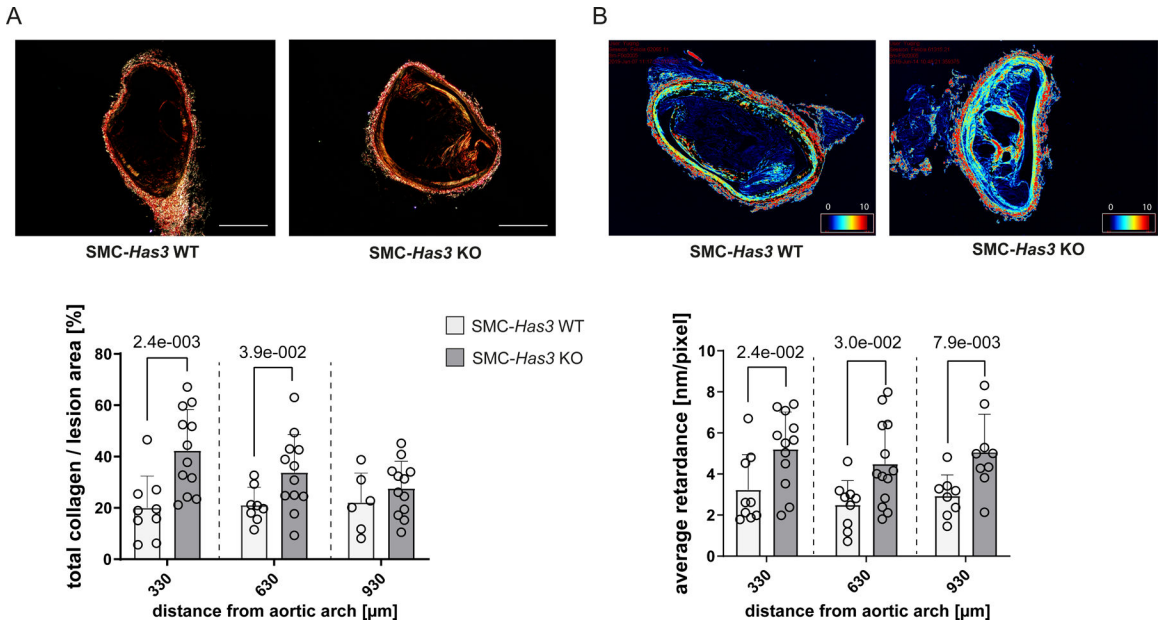

Fig. 2: SMC-specific KO of *Has3* results in increased collagen deposition and maturation in atherosclerotic lesions.

(A) Representative images of Picrosirius red stained BCAs under polarized light and analysis of total collagen deposition in atherosclerotic plaque lesions of SMC-*Has3* WT and SMC-*Has3* KO mice at three different locations along the BCA (n=9/12 (330 µm), n=8/12 (630 µm), n=6/12 (930 µm)). **(B)** Measurement of collagen orientation and alignment using LC-PolScope analysis, where well-aligned collagen fibers are birefringent and retard plane-polarized light. The heat map is proportional to retardance (nm/pixel) from low (black = 0 nm) to high (red = 10 nm) retardance (n=9/12 (330 µm), n=9/13 (630 µm), n=8/9 (930 µm)). Statistical analysis was performed separately at three different locations along the BCA with Mann-Whitney tests. Error bars represent mean ± SD. Scale bars = 500 µm.

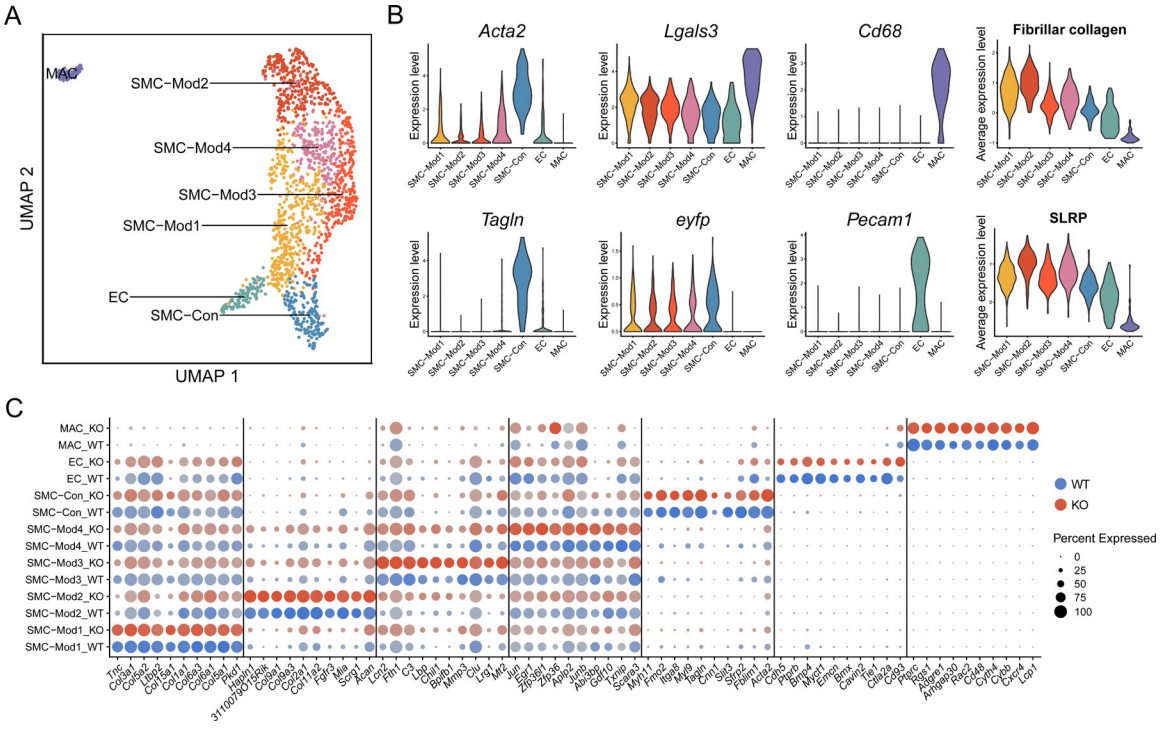

Fig. 3: Single-cell transcriptome profiling of advanced BCA lesions from SMC-*Has3* deficient mice and their respective littermates.

(A) UMAP visualization of aggregate SMC-*Has3* WT (WT) and SMC-*Has3* KO (KO) SMC-enriched cell populations of advanced BCA lesions after 15 weeks of western diet. **(B)** Expression of selected SMC, endothelial and macrophage markers, including gene signature scores for fibrillar collagens and SLRPs across cell identities for SMC-*Has3* WT and SMC-*Has3* KO mice, visualized using violin plots. Associated statistics can be found in Supplemental File 7. **(C)** Dot plot showing the expression of the top 10 conserved marker genes for each cell population broken down by genotype. EC; endothelial cell, MAC; macrophage, SLRPs; small leucine-rich proteoglycans, SMC; smooth muscle cell, UMAP; Uniform Manifold Approximation and Projection.

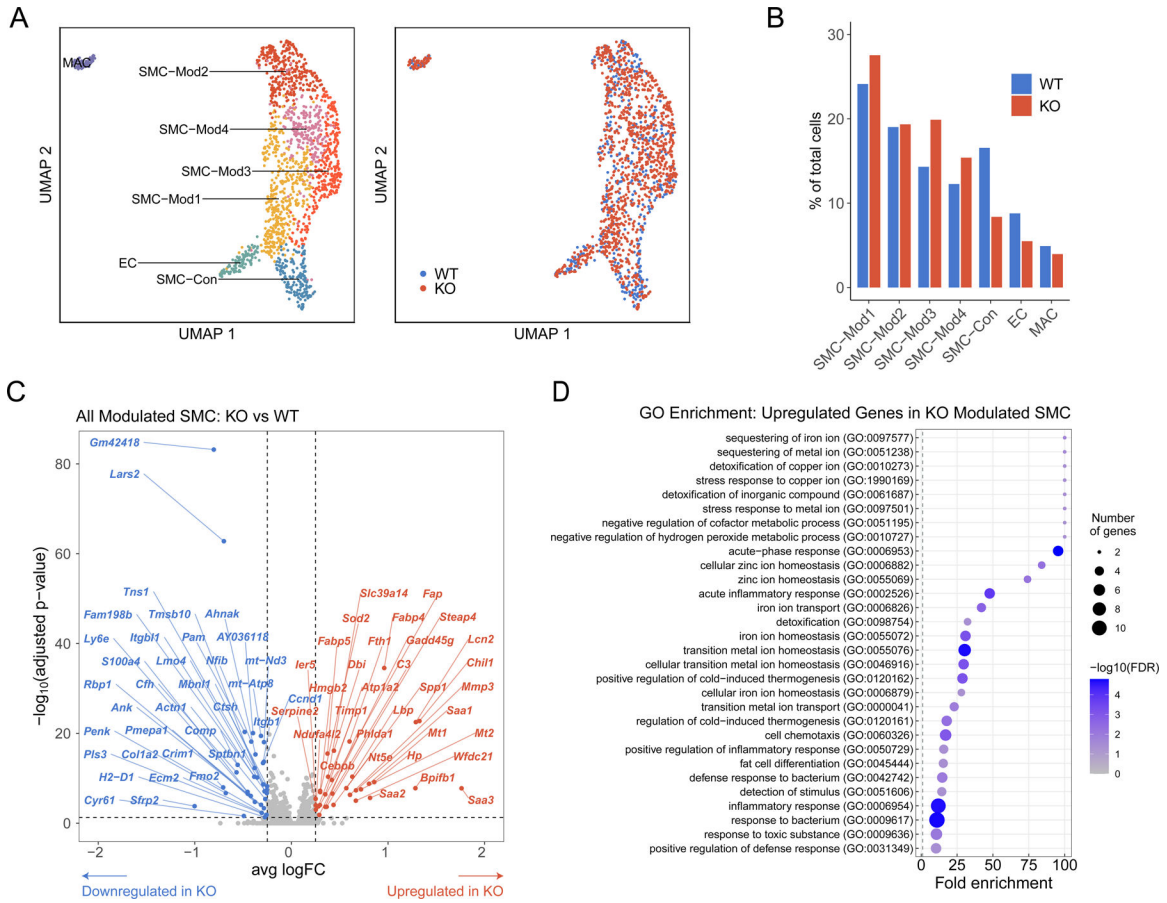

Fig. 4: scRNA-seq analysis of advanced BCA lesions shows that SMC-*Has3* KO is associated with enhanced SMC phenotypic modulation and acute-phase response gene expression.

(A) UMAP visualization of SMC-*Has3* WT (WT) and SMC-*Has3* KO (KO) cell distribution. **(B)** Proportion of each cell population as a percentage of the total cells in SMC-*Has3* WT and SMC-*Has3* KO data sets. **(C)** Differential gene expression analysis of all modulated SMC clusters, SMC-Mod1, SMC-Mod2, SMC-Mod3 and SMC-Mod4, from SMC-*Has3* KO mice compared with SMC-*Has3* WT mice, visualized by volcano plot. Significantly regulated genes are labeled, upregulated in SMC-*Has3* KO (red), downregulated in SMC-*Has3* KO (blue). **(D)** Gene ontology enrichment analysis (biological process), of upregulated genes in modulated SMC from SMC-*Has3* KO mice. EC; endothelial cell, FC; fold change, FDR; false discovery rate, GO; Gene ontology, MAC; macrophage, SMC; smooth muscle cell, UMAP; Uniform Manifold Approximation and Projection.

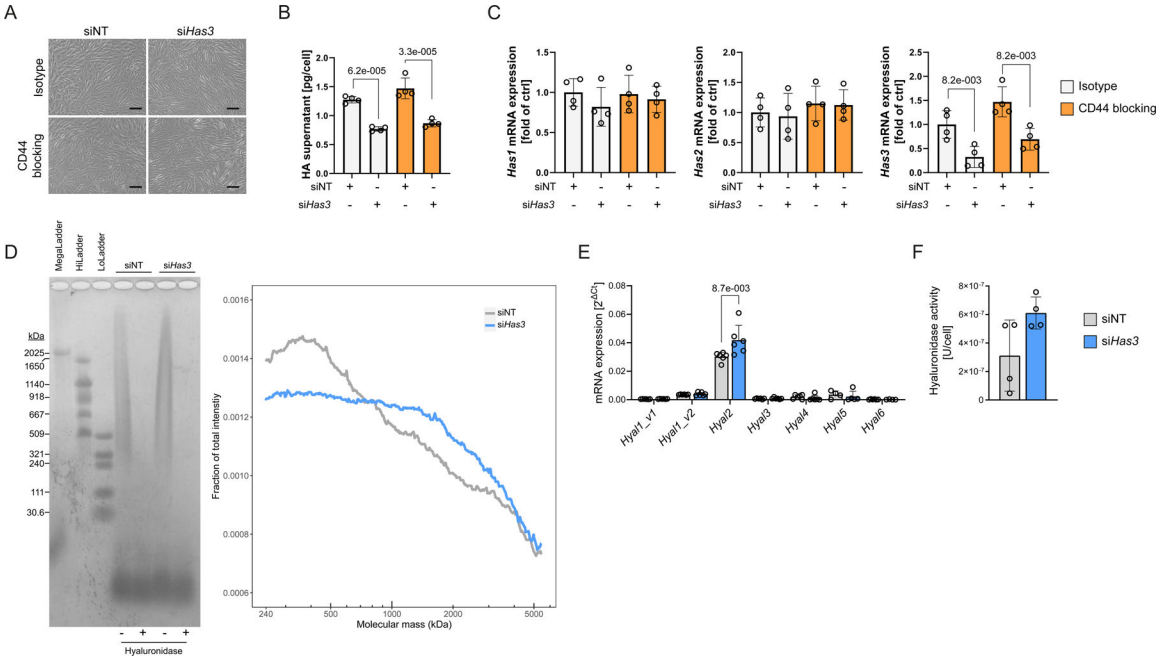

Fig. 5: Hyaluronan synthesis, molecular mass distribution and hyaluronidase activity in murine SMC after *Has3* knockdown.

Murine SMC cultures were stimulated with PDGF-BB and TGF-β1 followed by treatment with small interfering RNA against *Has3* and a CD44 blocking antibody. **(A)** No observable morphological differences. **(B-C)** Quantification of secreted HA and *Has* gene expression. **(D)** Molecular mass distribution of secreted HA. HA content was previously quantified and equal amounts were loaded in each lane. **(E)** Hyaluronidase gene expression. **(F)** Hyaluronidase activity of cell culture supernatant. Statistical analysis was performed with aligned rank transform (ART) ANOVA, post hoc pairwise multiple comparisons were adjusted with Sidak's correction (B, C) or Mann-Whitney test (E, F). Error bars represent mean ± SD, n=4/4 (B, C), n=6/6 (E), n=4/4 (F) technical independent samples. Scale bars = 100 μm.

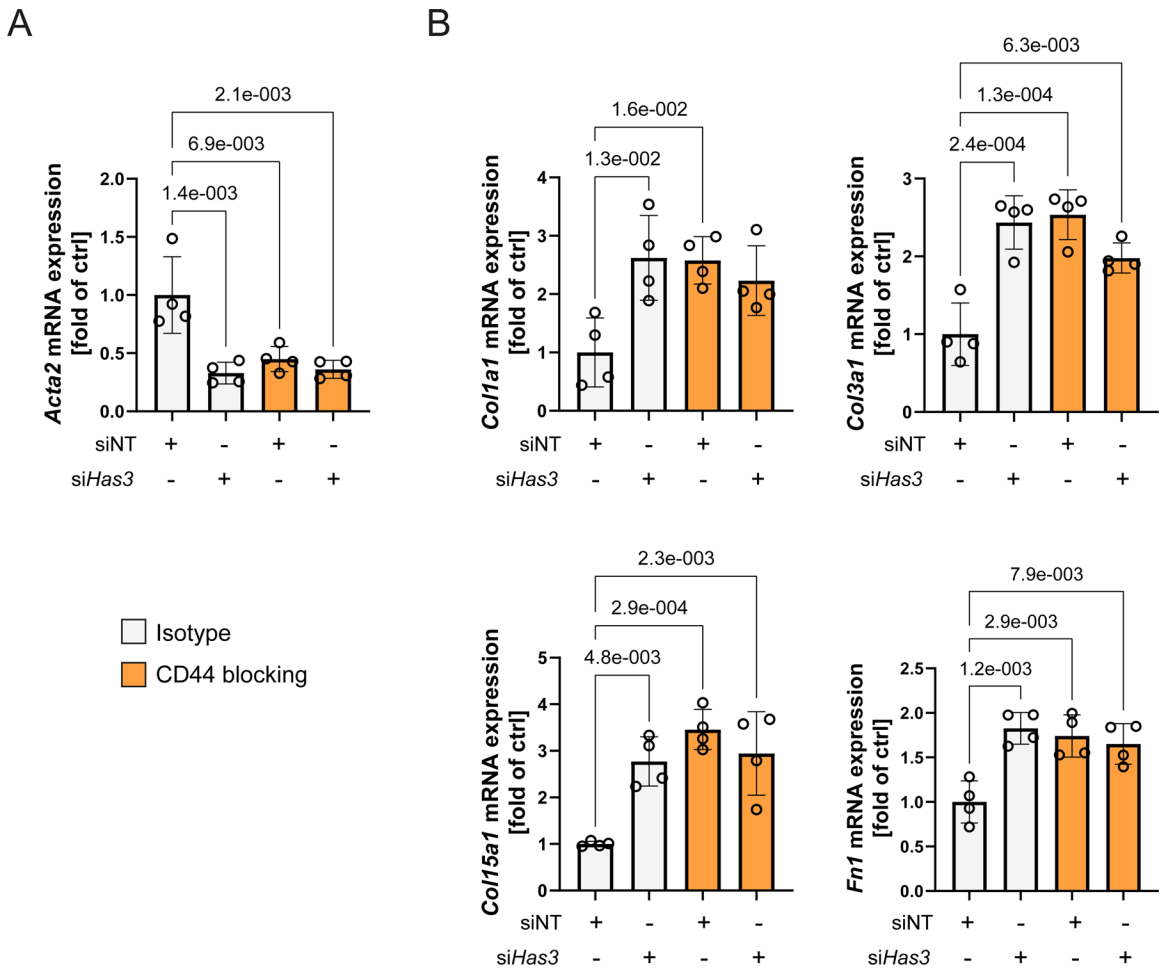

Fig. 6: *Has3* knockdown or CD44 blocking enhances a modulated phenotype in murine SMC *in vitro*.

Murine SMC cultures were stimulated with PDGF-BB and TGF-β1 followed by treatment with small interfering RNA against *Has3* and a CD44 blocking antibody. **(A)** *Has3* silencing and/or CD44 blocking reduces the expression of the contractile marker gene *Acta2*. **(B)** *Has3* silencing and/or CD44 blocking induces extracellular matrix gene expression (*Col1a1, Col3a1, Col15a1* and *Fn1*). No additive effects were observed with simultaneous *Has3* silencing and CD44 blocking. Statistical analysis was performed with two-way ANOVA, post hoc pairwise multiple comparisons were adjusted with Sidak's correction. Error bars represent mean ± SD, n=4/4, technical independent samples.

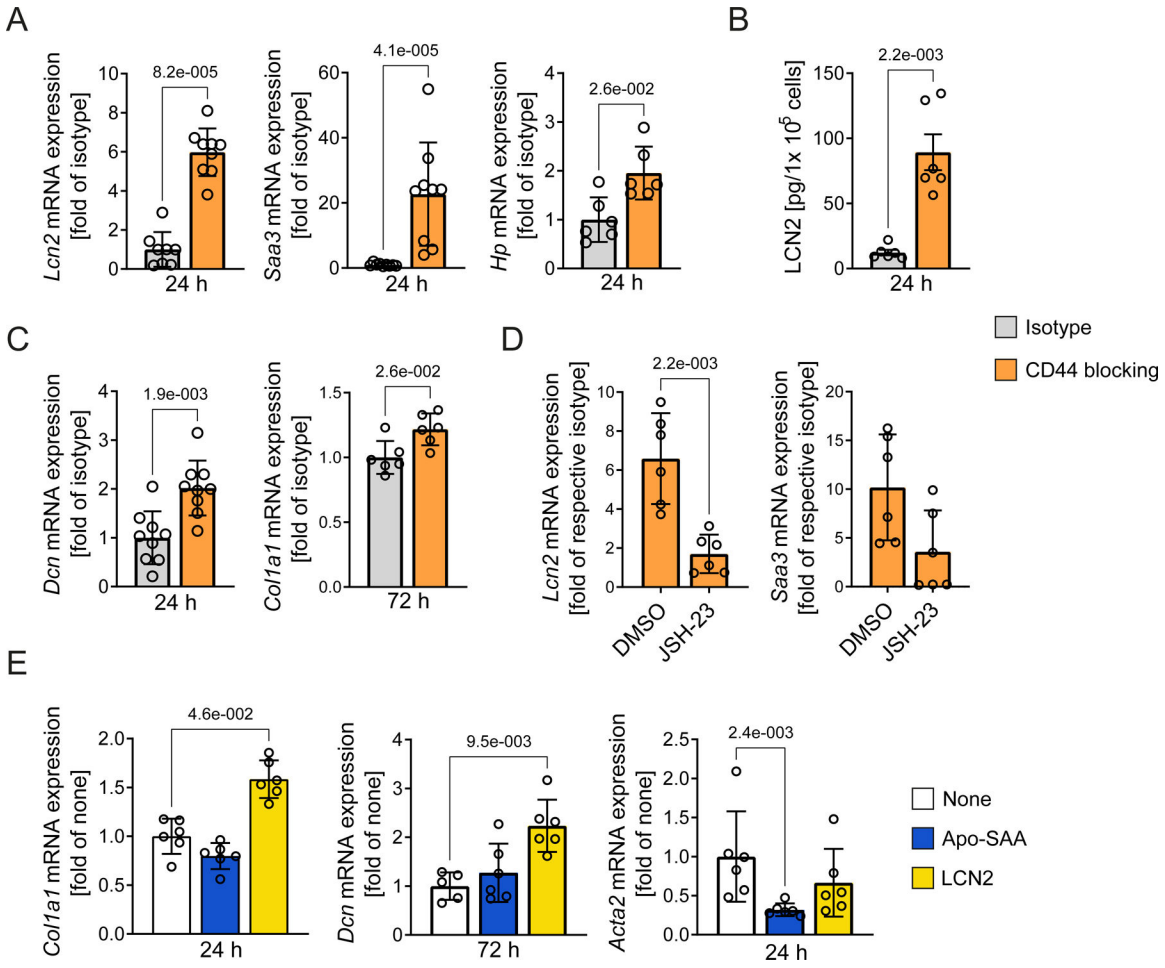

Fig. 7: CD44 blocking in murine SMC induces acute-phase protein gene expression which drives phenotypic modulation.

Murine SMC cultures were treated with a CD44 blocking antibody or recombinant acute-phase response proteins, without previous growth factor stimulation. **(A)** mRNA expression of acute-phase response genes (*Lcn2,* n=8/9*; Saa3*, n=8/9; and *Hp,* n=6/6*)*, is upregulated in response to CD44 blocking compared to isotype control. **(B)** LCN2 protein quantification via ELISA of the cell culture supernatant (n=6/6). **(C)** Fibrotic gene expression (*Col1a1,* n=9/9 and *Dcn,* n=6/6) is upregulated in response to CD44 blocking. **(D)** Acute-phase response gene expression stimulated by CD44 blocking is blunted by the NF-κB translocation inhibitor JSH-23 (10 μM) (n=6/6). **(E)** Stimulation of murine SMC with recombinant acute-phase proteins induces *Col1a1* and *Dcn* expression (LCN2, 1 μg/mL) and downregulates *Acta2* (Apo-SAA, 6.5 μg/mL) (n=6/6). Statistical analysis was performed with Mann-Whitney tests (A-D) or Kruskal-Wallis (E), post hoc pairwise multiple comparisons were adjusted with Dunn's correction. Error bars represent mean ± SD.

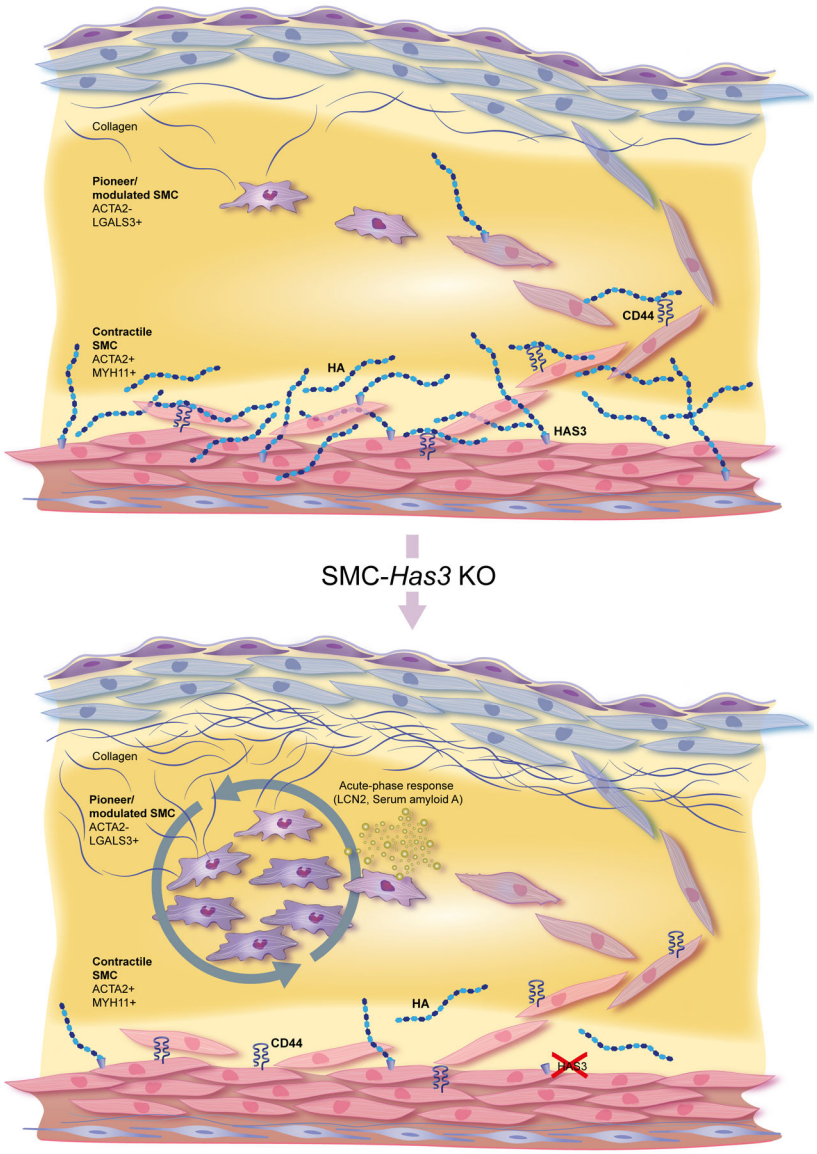

Fig. 8: Schematic overview.

HA is known to have a crucial influence on volume expansion in atherosclerotic lesion development as well as SMC proliferation and migration. HAS3 is a strong contributor to HA deposition in early lesion development. Immunostaining of SMC-*Has3* KO mice revealed an increase in LGALS3^{+} pioneering/modulated SMC which contribute to collagen deposition and maturation within the lesion and the fibrous cap. Single-cell RNA sequencing of BCA lesions and *in vitro* analysis of murine SMC revealed this phenotype is driven by an excessive acute-phase response by SMC, which may drive phenotypic modulation. Presumably, under normal conditions, HA/CD44 interaction serves to negatively regulate the acute-phase response of SMC, and therefore controls phenotypic switching during the progression of atherosclerosis.

Major Resources Table

Animals (in vivo studies)				
Species	**Vendor or Source**	**Background Strain**	**Sex**	**Persistent ID / URL**
Mouse	self breeding, Owens Lab CVRC, UVA	*Myh11*-CreER^{T2} ROSA26-STOP floxed *e*YFP *Apoe*$^{-/-}$ X *HAS3*$^{fl/fl}$	male	PMID: 18084302 https://www.genoway.com/

Genetically Modified Animals					
	Species	**Vendor or Source**	**Background Strain**	**Other Information**	**Persistent ID / URL**
Parent - Male	see table above	-	-	-	-
Parent - Female	-	-	-	-	-

Antibodies					
Target antigen	**Vendor or Source**	**Catalog #**	**Working concentrati on**	**Lot # (preferred but not required)**	**Persistent ID / URL**
TER119	Rat anti mouse	sc-19592	1 µg/mL	-	https://www.scbt.com/p/erythroid-lineage-antibody-ter-119?productCanUrl=erythroid-lineage-antibody-ter-119&_requestid=1812813
DCN	Rabbit anti mouse	LF113	1 µg/mL	-	Larry Fisher Lab
GFP	Goat polyclonal anti-GFP	ab6673	4 µg/mL	-	https://www.abcam.com/gfp-antibody-ab6673.html
LGALS3	Rat anti mouse	CL8942A P	2 µg/mL	-	https://dev.cedarlanelabs.com/products/detail/cl8942ap
ACTA2	Mouse monoclon al SM α-actin-FITC	C6198	4.4 µg/mL	-	https://www.sigmaaldrich.com/catalog/product/sigma/c6198?lang=de&region=DE
	Goat anti-rabbit IgG-HRP	sc2004	1 µg/mL	-	https://www.scbt.com/p/goat-anti-rabbit-igg-hrp
	Donkey anti-rat IgG-Dylite-550	ab102261	1:100	-	https://www.abcam.com/donkey-rat-igg-hl-dylight-550-preadsorbed-ab102261.html
	Donkey anti-goat 647	A21447	1:100	-	https://www.thermofisher.com/antibody/product/Donkey-anti-Goat-IgG-H-L-Cross-Adsorbed-Secondary-Antibody-Polyclonal/A-21447
CD44	KM201	1500–01	10 µg/mL	-	https://www.southernbiotech.com/ProductSearch.aspx?kwd=1500–01
IgG1κ isotype control	-	0116–01	10 µg/mL	-	https://www.southernbiotech.com/productsearch.aspx?cid=0116–01

DNA/cDNA Clones			
Clone Name	**Sequence**	**Source / Repository**	**Persistent ID / URL**
si*Has3*	sense Has3 siRNA: 5 ´AGGUGGUCAUGGUAGUGGAtt-3´ antisense Has3 siRNA: 5´-UCCACUACCAUGACCACCUtg −3´	# 4390771	https://www.thermofisher.com/order/genome-database/details/sirna/s67372?CID=&ICID=&subtype=sirna_silencer_select
siNT	-	# 4390844	https://www.thermofisher.com/order/catalog/product/4390843#/4390843

Cultured Cells			
Name	**Vendor or Source**	**Sex (F, M, or unknown)**	**Persistent ID / URL**
Aortic murine SMC, passages 7–12	self-made cell line, Owens Lab CVRC, UVA	unknown	-

Data & Code Availability		
Description	**Source / Repository**	**Persistent ID / URL**

Other		
Description	**Source / Repository**	**Persistent ID / URL**
DAPI dye, 0.05 mg/mL	# D3571	https://www.thermofisher.com/order/catalog/product/D3571#/D3571
HABP, 1:150	# 385911	https://www.sigmaaldrich.com/catalog/product/mm/385911?lang=en&region=US
Streptavidin Alexa Fluor 488, 1:100	# S11223	https://www.thermofisher.com/order/catalog/product/S11223#/S11223
Recombinant Apo-SAA, 6.5 μg/mL	# 300–13	https://www.peprotech.com/de/recombinant-human-apo-saa
Recombinant Lipocalin-2, 10 μg/mL	# 1857-LC-050	https://www.rndsystems.com/products/recombinant-mouse-lipocalin-2-ngal-protein-cf_1857-lc
JSH-23, 10 μM	# J4455–5MG	https://www.sigmaaldrich.com/DE/de/product/sigma/j4455?context=product
HABP ELISA-like assay		Corgenix Medical Corporation
mouse Lipocalin-2 ELISA kit	# ab199083	https://www.abcam.com/mouse-lipocalin-2-elisa-kit-ngal-ab199083.html
Hyaluronidase Activity ELISA	# K-6000	https://echelon-inc.com/product/hyaluronidase-activity-elisa/
Streptomyces Hyaluronidase	# 389561	https://www.emdmillipore.com/US/en/product/Hyaluronidase-Streptomyces-hyaluronlyticus-nov.-sp.,EMD_BIO-389561?ReferrerURL=https%3A%2F%2Fwww.google.com%2F